The Canadian Mineralogist
Vol. 47, pp. 173-180 (2009)
DOI: 10.3749/canmin.47.1.173

THE CRYSTAL STRUCTURE OF ERCITITE, $Na_2(H_2O)_4[Mn^{3+}{}_2(OH)_2(PO_4)_2]$, AND ITS RELATION TO BERMANITE, $Mn^{2+}(H_2O)_4[Mn^{3+}{}_2(OH)_2(PO_4)_2]$

MARK A. COOPER, FRANK C. HAWTHORNE§ AND PETR ČERNÝ

Department of Geological Sciences, University of Manitoba, Winnipeg, Manitoba R3T 2N2, Canada

ABSTRACT

The crystal structure of ercitite, ideally $Na_2(H_2O)_4[Mn^{3+}{}_2(OH)_2(PO_4)_2]$, orthorhombic, *a* 6.2499(6), *b* 8.7479(9), *c* 19.9554(17) Å, *V* 1091.0 Å^3, space group *Cmca*, *Z* = 4, D_{calc} = 2.77 g.cm^{-3}, from the Tanco granitic pegmatite, Bernic Lake, southeastern Manitoba, Canada, has been solved by direct methods and refined to R_1 = 4.0% on the basis of 431 unique observed reflections $|F_o \geq 4\sigma F|$ collected on a Bruker *P*4 diffractometer equipped with a CCD 1K Smart detector and Mo$K\alpha$ radiation. There is one distinct *P* site occupied by P and coordinated by four O atoms in an tetrahedral arrangement, with a <*P*–O> distance of 1.541 Å. There are two octahedrally coordinated *M* sites: *M*(1) is occupied by $(Mn^{3+}{}_{0.53}Fe^{3+}{}_{0.46}Al_{0.01})$ with a <*M*(1)–O> distance of 2.028 Å, and *M*(2) is occupied by $(\square_{0.93}Mn^{2+}{}_{0.07})$ with a <*M*(2)–O> distance of 2.252 Å. The *M*(1) octahedron shows four short meridional bonds (~1.95 Å) and two long apical bonds (2.176 Å) characteristic of Jahn–Teller-distorted octahedrally coordinated Mn^{3+}. There is one distinct *Na* site occupied by $(Na_{0.89}Ca_{0.04}\square_{0.07})$ and coordinated by six anions with a <*Na*–O> distance of 2.504 Å. The structural unit in ercitite, $[Mn^{3+}{}_2(OH)_2(PO_4)_2]$, is chemically and topologically identical to the structural unit in bermanite, $Mn^{2+}(H_2O)_4[Mn^{3+}{}_2(OH)_2(PO_4)_2]$. However, the stacking of these sheet-like units differs between the two minerals; the sheets in ercitite link through corner-sharing of [7]-coordinated Na polyhedra that share edges with the polyhedra of the structural units, whereas the sheets in bermanite link by sharing polyhedron corners with interstitial $\{Mn^{2+}O_2(H_2O)_4\}$ octahedra.

Keywords: ercitite, bermanite, crystal structure, phosphate.

SOMMAIRE

La structure cristalline de l'ercitite, de composition idéale $Na_2(H_2O)_4[Mn^{3+}{}_2(OH)_2(PO_4)_2]$, orthorhombique, *a* 6.2499(6), *b* 8.7479(9), *c* 19.9554(17) Å, *V* 1091.0 Å^3, groupe spatial *Cmca*, *Z* = 4, D_{calc} = 2.77 g.cm^{-3}, provenant de la pegmatite granitique de Tanco, au lac Bernic, dans le sud-est du Manitoba, Canada, a été résolue par méthodes directes et affinée jusqu'à un résidu R_1 de 4.0% en utilisant 431 réflexions uniques observées $|F_o \geq 4\sigma F|$ prélevées avec un diffractomètre Bruker *P*4 muni d'un détecteur CCD 1K Smart et avec rayonnement Mo$K\alpha$. La structure contient un site *P* distinct qu'occupe les atomes P entourés de quatre atomes d'oxygène formant un tétraèdre, avec une distance <*P*–O> de 1.541 Å. Elle contient deux sites *M* à coordinence octaédrique: *M*(1) a une occupation $(Mn^{3+}{}_{0.53}Fe^{3+}{}_{0.46}Al_{0.01})$ avec une distance <*M*(1)–O> de 2.028 Å, et *M*(2) contient $(\square_{0.93}Mn^{2+}{}_{0.07})$, avec une distance <*M*(2)–O> de 2.252 Å. L'octaèdre *M*(1) possède quatre liaisons méridionales courtes (~1.95 Å) et deux liaisons plus longues avec les sommets (2.176 Å), ce qui caractérise les octaèdres difformes contenant le Mn^{3+}, à cause de l'effet Jahn–Teller. Il y a de plus un site distinct *Na* où loge $(Na_{0.89}Ca_{0.04}\square_{0.07})$, coordonné par six anions avec une distance <*Na*–O> de 2.504 Å. Le module structural de l'ercitite, $[Mn^{3+}{}_2(OH)_2(PO_4)_2]$, est chimiquement et topologiquement identique à celui de la bermanite, $Mn^{2+}(H_2O)_4[Mn^{3+}{}_2(OH)_2(PO_4)_2]$. Toutefois, le mode d'empilement des feuillets dans ces deux minéraux diffère; les feuillets de l'ercitite sont agencés par partage de coins des polyèdres Na à coordinence [7], qui partagent des arêtes avec les polyèdres des modules structuraux, tandis que les feuillets de la bermanite sont liés par partage de coins de polyèdres avec les octaèdres $\{Mn^{2+}O_2(H_2O)_4\}$interstitiels.

(Traduit par la Rédaction)

Mots-clés: ercitite, bermanite, structure cristalline, phosphate.

§ *E-mail address*: frank_hawthorne@umanitoba.ca

Introduction

Ercitite, a Mn phosphate mineral of ideal composition $Na_2(H_2O)_4[Mn^{3+}{}_2(OH)_2(PO_4)_2]$, was reported from the Tanco granitic pegmatite in Manitoba, Canada, where it occurs as a brownish black crust on lithiophilite (Fransolet *et al*. 2000). Preliminary crystal-structure work indicated that the structure of ercitite is related to that of bermanite, $Mn^{2+}(H_2O)_4[Mn^{3+}{}_2(OH)_2(PO_4)_2]$ (Kampf & Moore 1976), but problems with crystal size and quality precluded a good refinement of its structure at that time. We persisted with this work as the chemical relation between these two minerals, $Na + Na \leftrightarrow Mn^{2+} + \square$, did not suggest a simple replacement substitution in the bermanite-type structure. We present the results of this work here.

Experimental

Data collection

Ercitite forms fan-like divergent sprays of lath-like crystals that are of poor quality with regard to diffraction. After considerable effort, we found a crystal adequate for the collection of single-crystal X-ray intensity data. This crystal was also used to collect the optical and structural data for the original description by Fransolet *et al*. (2000). We did not microprobe this particular crystal as it was the only crystal adequate for collection of single-crystal X-ray-diffraction data, and we did not wish to destroy it. The chemical analysis of Fransolet *et al*. (2000) was done on a small fragment associated with the crystal used for diffraction and optical measurements. The crystal was attached to a tapered glass fiber and mounted on a Bruker *P*4 diffractometer equipped with a serial detector and graphite-filtered Mo*K*α X-radiation. The diffracted intensities were found to be weak, and little was observed above 45° 2θ, even though we used a fixed scan-speed of 0.50° per minute. A total of 837 intensities was collected, and 482 of these had $|F_o| > 4\sigma F$. The data were indexed on a monoclinic cell, following the chemical similarity to bermanite, but this cell is easily transformed to conform with orthorhombic symmetry. We could not collect adequate psi-scan data for an absorption correction. However, the data did allow confirmation of a structure topologically similar to that of bermanite. Acquisition of a SMART 1K area detector encouraged us to recollect intensity data because of the resulting increased sensitivity. We observed a second weak component in the complete diffraction pattern, with a small angular displacement from the main pattern. The intensities of 3272 reflections from the main pattern were collected to 50° 2θ using 120 s per 0.2° frame. The cell dimensions were determined from 2369 reflections with $I > 10\sigma I$, initially as monoclinic, but again this cell is easily transformed to conform with orthorhombic symmetry. The intensity data were integrated on two different cells, of orthorhombic and monoclinic symmetry, respectively, and processed with Sadabs (Sheldrick 1998). The diffraction pattern is compatible with space groups *Cmca* and $P2_1/n$, respectively, and the corresponding refined cell-dimensions are given in Table 1. There were four (two) reflections not consistent with the symmetry *Cmca* ($P2_1/n$) at the 3σ level, and zero for both at the 4σ level. The data were corrected for absorption, Lorentz, polarization and background effects, averaged and reduced to structure factors. Other information pertinent to data collection is given in Table 1.

TABLE 1. MISCELLANEOUS CRYSTALLOGRAPHIC AND REFINEMENT INFORMATION ABOUT ERCITITE

	Cmca	$P2_1/n$
a (Å)	6.2499(6)	5.3757(5)
b	8.7479(9)	19.9553(17)
c	19.9554(17)	5.3750(5)
β (°)		108.915(2)
V (Å^3)	1091.0(3)	545.5(2)
Z	4	2
$D_{calc.}$ (g/cm^3)	2.77	
Crystal size (mm)	0.005 × 0.040 × 0.160	
Radiation/filter	Mo*K*α/graphite	
2θ limit	50	
No. of reflections	3272	
Unique/observed reflections	537/431	971/716
R_{merge} (%)	5.0	4.6
Refinement method	full-matrix least squares on F^2	
Goodness of fit on F^2	1.10	1.12
Final $R_{(obs)}$ (%) [$\|F_o\| > 4\sigma F$]	4.0	4.7
R_1 (all data) (%)	5.3	7.0
wR_2 (all data) (%)	9.9	11.6

Structure refinement

The crystal structure of ercitite was refined with the Bruker Shelxtl Version 5.1 system of programs (Sheldrick 1997). Scattering curves for neutral atoms were taken from the International Tables for Crystallography (1992). We decided to refine the structure in both space groups to test the efficacy of each. Full-matrix least-squares refinement converged rapidly to R_1 indices of ~5%. At this stage, difference-Fourier maps showed the presence of an additional center of electron density in both space groups. The associated interatomic distances are compatible with occupancy of this site by Mn^{2+}, and an additional site, *M*(2) occupied by Mn, was introduced into the refinement, with the occupancy considered as variable in the refinement. The results of refinement in each space group are given in Table 1. All final *R* indices are lower for *Cmca* than for $P2_1/n$, despite the greater number of degrees of freedom for the latter symmetry, and hence we adopted the space group *Cmca*. Details of the structure refinement are given in Table 1, final atom parameters in Table 2, selected interatomic distances and angles in Table 3, and bond valences in Table 4. A table of structure factors is available from the Depository of Unpublished Data on the MAC website [document Ercitite CM47_173].

TABLE 2. ATOM POSITIONS AND DISPLACEMENT PARAMETERS FOR ERCITITE

	x	*y*	*z*	U_{eq}	U_{11}	U_{22}	U_{33}	U_{23}	U_{13}	U_{12}
P	½	0.4767(2)	0.09528(10)	0.0093(5)	0.0102(9)	0.0085(10)	0.0093(9)	–0.0009(8)	0	0
M(1)	¼	¼	½	0.0097(3)	0.0075(5)	0.0119(6)	0.0097(5)	0.0011(5)	–0.0003(5)	0.0001(5)
M(2)	¾	0.560(2)	¼	0.029(7)	0.034(12)	0.033(11)	0.018(10)	0	0.004(9)	0
Na	½	0.3132(4)	0.34717(16)	0.0205(8)	0.0183(17)	0.0275(19)	0.0155(16)	0.0045(15)	0	0
O(1)	½	0.6282(6)	0.540(3)	0.0154(13)	0.025(3)	0.013(3)	0.009(3)	0.001(2)	0	0
O(2)(OH)	½	0.3673(6)	0.5267(3)	0.0093(11)	0.009(3)	0.008(3)	0.011(3)	0.001(2)	0	0
O(3)	½	0.5198(7)	0.1688(3)	0.0184(13)	0.022(3)	0.026(3)	0.007(3)	–0.002(3)	0	0
O(4)	0.2976(6)	0.3845(4)	0.07732(17)	0.0119(9)	0.008(2)	0.0156(19)	0.0117(17)	–0.0030(15)	0.0003(15)	0.0003(15)
O(5)(H_2O)	¾	0.3280(8)	¼	0.0344(16)	0.018(3)	0.063(5)	0.022(3)	0	–0.002(3)	0
O(6)(H_2O)	½	0.5921(7)	0.3326(3)	0.0235(15)	0.023(3)	0.026(4)	0.022(3)	–0.001(3)	0	0
H(1)	0.648(8)	0.3936(12)	0.226(3)	0.1*						
H(2)	0.6272(9)	0.650(5)	0.319(4)	0.1*						

* constrained in refinement.

TABLE 3. SELECTED INTERATOMIC DISTANCES (Å) AND ANGLES (°) IN ERCITITE

P – O(1)		1.561(6)		*M*(1) – O(1)b,c	×2	2.176(4)	
P – O(3)		1.515(5)		*M*(1) – O(2),d	×2	1.944(3)	
P – O(4),a	×2	1.543(4)		*M*(1) – O(4)e,f	×2	1.963(3)	
<*P*–O>		1.541		<*M*(1)–O>		2.028	
M(2) – O(3),g	×2	2.278(5)		*Na* – O(1)b		2.551(6)	
M(2) – O(5)		2.03(2)		*Na* – O(3)b		2.586(7)	
M(2) – O(5),i		2.35(2)		*Na* – O(4)e,g	×2	2.473(4)	
M(2) – O(6),l	×2	2.289(5)		*Na* – O(5),h	×2	2.494(3)	
<*M*(2)–O>		2.252		*Na* – O(6)		2.457(7)	
				<*Na*–O>		2.504	
O(2)...O(6)j	2.830(8)						
O(5)–H(1)	0.98(1)	H(1)…O(3)	1.841(18)	O(5)…O(3)		2.807(7)	
O(5)–H(1)k	0.98(1)	H(1)k…O(3)g	1.841(18)	O(5)…O(3)g		2.807(7)	
H(1)–O(5)–H(1)k	108(4)	O(5)–H(1)–O(3)	168(7)	O(5)–H(1)k–O(3)g		168(7)	
O(6)–H(2)	0.98(1)	H(2)…O(5)i	2.22(2)	O(6)…O(5)i		3.069(7)	
O(6)–H(2)a	0.98(1)	H(2)a…O(5)l	2.22(2)	O(6)…O(5)l		3.069(7)	
H(2)–O(6)–H(2)a	108(4)	O(6)–H(2)–O(5)i	145(3)	O(6)–H(2)a–O(5)l		145(3)	

Symmetry positions: a: $\bar{x}$ + 1, *y*, *z*; b: *x*, *y* – ½, $\bar{z}$ + ½; c: $\bar{x}$ + ½, $\bar{y}$ + 1, z + ½; d: $\bar{x}$ + ½, $\bar{y}$ + ½, $\bar{z}$ + 1; e: $\bar{x}$ + ½, *y*, $\bar{z}$ + ½; f: *x*, $\bar{y}$ + ½, *z* + ½; g: *x* + ½, *y*, $\bar{z}$ + ½; h: *x* – ½, *y*, $\bar{z}$ + ½; i: *x*, *y* + ½, $\bar{z}$ + ½; j: $\bar{x}$ + 1, $\bar{y}$ + 1, $\bar{z}$ + 1; k: $\bar{x}$ + $^3/_2$, *y*, $\bar{z}$ + ½; l: $\bar{x}$ + 1, *y* + ½, *z*.

DESCRIPTION OF THE STRUCTURE

Cation sites

There is one *P* site, which is occupied by P with a coordination number of [4] and a <P–O> distance of 1.541 Å, close to the grand <P–O> distance of 1.537 Å reported for phosphate minerals by Huminicki & Hawthorne (2002). There are two *Mn* sites with a coordination number of [6], and <*Mn*–O> distances of 2.028 and 2.252 Å, respectively. Fransolet *et al.* (2000) gave the chemical composition of ercitite as $(Na_{0.89}Ca_{0.04})_{\Sigma 0.93}$ $(Mn^{3+}_{0.53}Fe^{3+}_{0.46}Al_{0.01})_{\Sigma 1.00}$ $(PO_4)_{1.01}$ (OH) $(H_2O)_2$. Site-scattering refinement gave the following values: *Na*: 21.6; *M*(1): 47.4; *M*(2): 3.6 *epfu* for *Z* = 4, in close accord with the calculated site-scattering from the electron-microprobe results: *Na*: 21.2; *M*(1) + *M*(2): 50.7 *epfu*. These results indicate that the *M*(1) site is occupied by $(Mn^{3+}_{0.53}Fe^{3+}_{0.46}Al_{0.01})$, and the mean bond-length is in accord with this assignment of formal valences. In a holosymmetric configuration, octahedrally coordinated Mn^{3+} has an electronically degenerate e_g electronic state. The Jahn–Teller theorem (Jahn & Teller 1937) indicates that such an octahedron is unstable with respect to some distorted state, and that a spontaneous distortion of the octahedron will

occur. In accord with the Jahn–Teller theorem, the *M*(1) octahedron in ercitite shows the typical [4 + 2]-coordination of Mn^{3+} with four short meridional bonds (~1.95 Å) and two long apical bonds (2.176 Å, Table 3), despite being occupied 0.53 Mn^{3+} + 0.46 Fe^{3+} + 0.01 Al (Fransolet *et al*. 2000). The distortion theorem of bond-valence theory (Brown 1981) indicates that the variation in mean bond-length in a specific polyhedron correlates with the dispersion of the constituent bond-lengths. Burns *et al*. (1994) examined this issue with regard to octahedrally coordinated Mn^{3+} and showed that there is a strong correlation in this particular case. The *M*(1) octahedron in ercitite lies slightly above the correlation of Burns *et al*. (1994), as do the *M*(4) site in fredrikssonite and the *M*(3) site in pinakiolite (Moore & Araki 1974). These three polyhedra have significant occupancy by Fe^{3+} in addition to Mn^{3+}, and the curve of Burns *et al*. (1994) indicates that the effective radius of Mn^{3+} in an undistorted octahedron is 0.61 Å, significantly less that that of Fe^{3+} (0.645 Å, Shannon 1976). Hence the presence of Fe^{3+} will lead to a positive deviation from the curve of Burns *et al*. (1994), as is observed in ercitite.

The *M*(2) site is occupied by ($Mn_{0.07}\square_{0.93}$) (□ = vacancy), and the <*M*(2)–O> distance is 2.252 Å. Although the *M*(2) site is dominated by □, the <*M*(2)–O> distance is ideal for occupancy of that site by Mn^{2+}, suggesting that this assigned occupancy is correct. There is one distinct *Na* site coordinated by seven anions with a <*Na*–O> distance of 2.504 Å. Results of the chemical analysis (Fransolet *et al*. 2000) indicate that the *Na* site is occupied by ($Na_{0.89}Ca_{0.04}\square_{0.07}$), and the observed <*Na*–O> distance is in accord with occupancy by large alkali and alkaline-earth cations. Examination by LA–ICP–MS showed that no Li is present.

Anion sites

There are six distinct anion sites (Table 2). Incident bond-valence from the principal cations at the *P* and *M*(1) sites (Table 4) indicates that O(2) is occupied by an (OH) group, and O(5) and O(6) are occupied by (H_2O) groups. The constraint of electroneutrality requires that the remaining sites be occupied by O^{2-}. This is certainly apparent for O(1) and O(4), which are each [3]-coordinated by P, *M*(1) and Na with resulting incident bond-valences of 1.93 and 1.96 *vu*, respectively, in accord with the valence-sum rule. The O(3) anion is only [2]-coordinated by P and Na for an incident bond-valence sum of 1.44 *vu* (Table 4). However, O(3) is also an acceptor anion for two hydrogen bonds from the H(1) atom of the (H_2O) group at O(5) (Table 4), and its incident bond-valence sum is 1.94 *vu*, in accord with the valence-sum rule.

TABLE 4. BOND VALENCES* (*vu*) FOR ERCITITE

	P	*M*(1)	*Na*	Sum	H(1)	H(2)	H(3)′	Sum
O(1)	1.16	0.32 ×2↓→	0.13	1.93				1.93
O(2)		0.61 ×2↓→		1.22			0.80	2.02
O(3)	1.32		0.12	1.44	0.25 ×2→			1.94
O(4)	1.22 ×2↓	0.58 ×2↓	0.16 ×2↓	1.96				1.96
O(5)			0.15 ×2↓ ·	0.30	0.75 ×2 ·	0.15 ×2 ·		2.10
O(6)			0.17	0.17		0.85 ×2→	0.20	2.07
Sum	4.92	3.02	1.04		1.00	1.00	1.00	

* calculated from the curves of Brown (1981).

Hydrogen bonding

Two peaks in the difference-Fourier map were located near the (H_2O) groups at O(5) and O(6), and inserted into the refinement model as H positions constrained to lie 0.98 Å from the donor O-atom and 1.59 Å from the associated H site of the same (H_2O) group. The (H_2O) group at the O(5) site, special position 8*e*, involves the H(1) site at the general position 16*g*, and the (H_2O) group at the O(6) site, special position 8*f*, involves the H(2) site at the general position 16*g*. The O(2) anion bonds to two M(1) cations, and the resulting incident bond-valence (1.22 *vu*, Table 4) indicates that O(2) must be an (OH) group. Its associated H, denoted as H(3)' in Table 4, could not be located on the mirror plane (8*f*), and is likely disordered off the mirror (½,*y*,*z*). The H(1) atom attached to the (H_2O) group at O(5) hydrogen-bonds to the O(3) anion, and each O(3) anion receives two such hydrogen bonds. The H(2) atom attached to the (H_2O) group at O(6) hydrogen-bonds to a neighboring (H_2O) group at O(5), and each O(5) anion receives two such hydrogen bonds. The H(3)' atom attached to the (OH) group at O(2) hydrogen-bonds to the (H_2O) group at O(6) (Tables 3, 4).

Bond topology

As conjectured by Fransolet *et al*. (2000), the structure of ercitite is strongly related to that of bermanite. Indeed, the structural unit $[Mn^{3+}{}_2(OH)_2(PO_4)_2]$ is topologically identical in each structure. As shown in Figure 1a, $[^{[6]}Mn^{3+}(OH)_2(^{[4]}PO_4)]$ chains link by sharing tetrahedron vertices to form a $[(Mn^{3+}(OH)(PO_4)]$ sheet that constitutes the structural unit (Hawthorne 1983, 1985, 1990, 1994). The linkage is also shown in Figure 1b, where it is apparent that the linkage of octahedra and tetrahedra is similar to that exhibited by the $[M(TO_4)_2\Phi_n]$ chains in the structures of the kröhnkite $[Na_2Cu^{2+}(SO_4)_2(H_2O)_2$, Hawthorne & Ferguson 1975], talmessite $[Ca_2Mg(AsO_4)_2(H_2O)_2$, Catti *et al*. 1977] and fairfieldite $[Ca_2Mn^{2+}(PO_4)_2(H_2O)_2$, Fanfani *et al*. 1970] groups (Fleck & Kolitsch 2003, Fleck *et al*. 2002, Wildner & Stoilova 2003, Kolitsch & Fleck 2005, Herwig & Hawthorne 2006).

The relative stacking of the $[Mn^{3+}(OH)(PO_4)]$ sheets is different in ercitite and bermanite (Fig. 2). In ercitite,

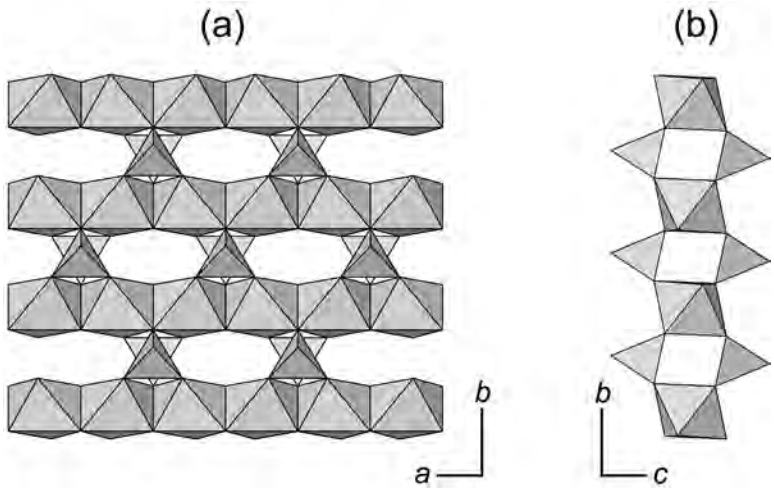

FIG. 1. The [$(Mn^{3+}(OH)(PO_4)$] sheet in ercitite (a) projected onto a plane close to (001), with the sheet tilted 5° about a horizontal axis to give a clearer view of the polyhedron linkage; (b) projected onto the (100) plane.

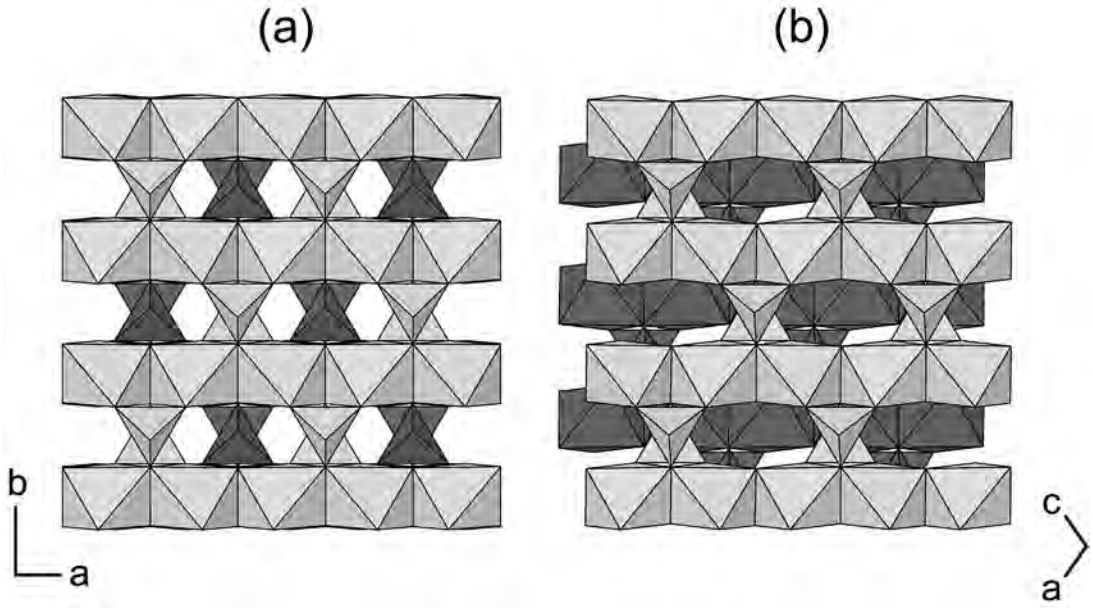

FIG. 2. Stacking of [$Mn^{3+}(OH)(PO_4)$] sheets in (a) ercitite projected down [001], and (b) bermanite projected down [010]. Dark grey polyhedra: lower layer; light grey polyhedra: upper layer.

the sheets of octahedra stack directly over each other with a lateral shift of "one octahedron" along [100] (Fig. 2a). In bermanite, adjacent sheets are offset, both along the chains and between the chains.

The attachment of the intersheet polyhedra to the upper surface of the [$Mn^{3+}(OH)(PO_4)$] sheet is shown in Figure 3, with the NaO_7 polyhedron in ercitite (Fig. 3a), and the $Mn^{2+}O_6$ octahedron in bermanite (Fig. 3b). In

both structures, the intersheet polyhedra are centered approximately over the central axis of the underlying Mn^{3+} chains. Although the lower $[Mn^{3+}(OH)(PO_4)]$ sheet is the same for the two structures, the positioning of the intersheet polyhedra along the Mn^{3+} chain-axis differs: in ercitite, the Na polyhedra nestle down among two Mn^{3+} octahedra and a PO_4 tetrahedron, sharing edges with these lower polyhedra (Figs. 3a, 4a); in bermanite, the Mn^{2+} octahedra lie above pairs of Mn^{3+} octahedra and share corners with (PO_4) tetrahedra (Figs. 3b, 4b). The connection between adjacent $[Mn^{3+}(OH)(PO_4)]$ sheets in ercitite occurs through the (H_2O) group at O(5) that bridges the Na polyhedra (Fig. 4a). In bermanite, the $[Mn^{3+}(OH)(PO_4)]$ sheets bridge through single Mn^{2+} octahedra *via trans* corner-sharing (Fig. 4b). Note that the relative offset in adjacent $[Mn^{3+}(OH)(PO_4)]$ sheets (shown in Fig. 2) can be viewed along the Mn^{3+} chains in Figure 4. The intersheet separation in ercitite (c = 19.96 Å) is larger than that in bermanite (b = 19.25 Å) by ~0.35 Å [*i.e.*, ($c_{ercitite} - b_{bermanite}$)/2].

The role of the M(2) site

In Figure 5, the mostly vacant $M(2)$ octahedron in ercitite is shown fully occupied and lying above the $[Mn^{3+}(OH)(PO_4)]$ sheet. Chains of edge-sharing $M(2)$ octahedra are centered over the region between the underlying chains of Mn^{3+} octahedra. Both the position and rotation of the $M(2)$ octahedron in ercitite differ from that of the Mn^{2+} intersheet octahedron in bermanite (Fig. 3b). In ercitite, minor occupancy of $M(2)$ by Mn^{2+} is accompanied by minor vacancy at the *Na* site (Fransolet *et al.* 2000). Moreover, the H sites associated with the (H_2O) groups bonded to intersheet

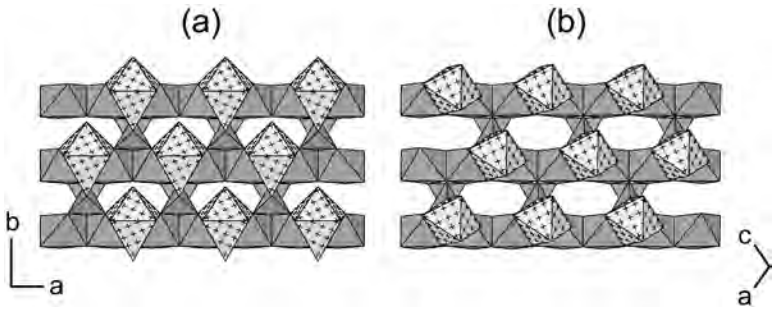

FIG. 3. Position of intersheet polyhedra (pale grey with crosses) above the $[Mn^{3+}(OH)(PO_4)]$ sheet (dark grey): (a) $^{[7]}$Na in ercitite projected down [001], (b) $^{[6]}Mn^{2+}$ in bermanite projected down [010].

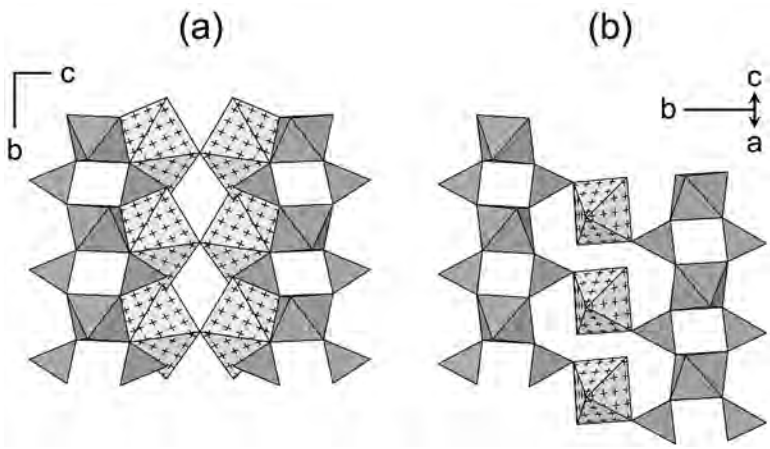

FIG. 4. Connectivity between $[Mn^{3+}(OH)(PO_4)]$ sheets in (a) ercitite projected down [100], and (b) bermanite projected down $[\bar{1}0\bar{1}]$. Legend as in Figure 3.

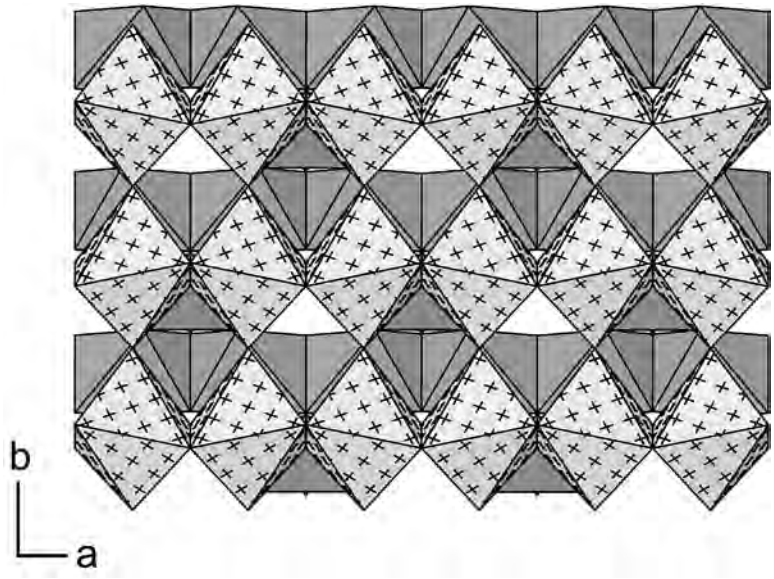

FIG. 5. Position of *M*(2) octahedra above the [$Mn^{3+}(OH)(PO_4)$] sheet in ercitite, projected down [001]. Legend as in Figure 3, light grey with crosses: *M*(2) octahedra.

Na are not compatible with occupancy of a neighboring *M*(2) site (by Mn^{2+}). Given that we also observed a second weak component in the complete diffraction pattern with a small angular displacement from the main pattern, we suggest the presence of an additional bermanite-like component in the crystal studied here.

Optical orientation and morphology

The earlier reported monoclinic cell (Fransolet *et al.* 2000) is transformed to the orthorhombic cell reported here *via* the matrix [1 0 1 / $\bar{1}$ 0 1 / 0 $\bar{1}$ 0], resulting in the following modifications to the description of the properties of ercitite: crystals elongated along [010] and flattened on {100}; two good cleavages on {100} and {001}; optical orientation X = *c*, Y = *b*, Z = *a*.

ACKNOWLEDGEMENTS

We thank Uwe Kolitsch, an anonymous reviewer, Associate Editor Encarna Roda and Editor Bob for their help with this manuscript. FCH was supported by a Canada Research Chair and Major Equipment, Discovery and Major Facilities Access grants from the Natural Sciences and Engineering Research Council of Canada, and by Innovation grants from the Canada Foundation for Innovation.

REFERENCES

BROWN, I.D. (1981): The bond-valence method: an empirical approach to chemical structure and bonding. *In* Structure and Bonding in Crystals II (M. O'Keeffe & A. Navrotsky, eds.). Academic Press, New York, N.Y. (1-30).

BURNS, P.C., COOPER, M.A. & HAWTHORNE, F.C. (1994): Jahn–Teller distorted $Mn^{3+}O_6$ octahedra in fredrikssonite, the fourth polymorph of $Mg_2Mn^{3+}(BO_3)O_2$. *Can. Mineral.* **32**, 397-403.

CATTI, M., FERRARIS, G. & IVALDI, G. (1977): Hydrogen bonding in the crystalline state. Structure of talmessite, $Ca_2(Mg,Co)(AsO_4)\bullet 2H_2O$, and crystal chemistry of related minerals. *Bull. Soc. fr. Minéral. Cristallogr.* **100**, 230-236.

FANFANI, L., NUNZI, A. & ZANAZZI, P.F. (1970): The crystal structure of fairfieldite. *Acta Crystallogr.* **B26**, 640-645.

FLECK, M. & KOLITSCH, U. (2003): Natural and synthetic compounds with kröhnkite-type chains. An update. *Z. Kristallogr.* **218**, 553-567.

FLECK, M., KOLITSCH, U. & HERTWECK, B. (2002): Natural and synthetic compounds with kröhnkite-type chains: review and classification. *Z. Kristallogr.* **217**, 435-443.

FRANSOLET, A.-M., COOPER, M.A., ČERNÝ, P., HAWTHORNE, F.C., CHAPMAN, R. & GRICE, J.D. (2000): The Tanco pegmatite at Bernic Lake, southeastern Manitoba. XV. Ercitite, $Na\ Mn^{3+}\ (PO_4)\ (OH)\ (H_2O)_2$, a new phosphate mineral species. *Can. Mineral.* **38**, 893-898.

HAWTHORNE, F.C. (1983): Graphical enumeration of polyhedral clusters. *Acta Crystallogr.* **A39**, 724-736.

HAWTHORNE, F.C. (1985): Towards a structural classification of minerals: the $^{VI}M\,^{IV}T_2\phi_n$ minerals. *Am. Mineral.* **70**, 455-473.

HAWTHORNE, F.C. (1990): Structural hierarchy in $^{[6]}M\,^{[4]}T\phi_n$ minerals. *Z. Kristallogr.* **192**, 1-52.

HAWTHORNE, F.C. (1994): Structural aspects of oxides and oxysalt crystals. *Acta Crystallogr.* **B50**, 481-510.

HAWTHORNE, F.C & FERGUSON, R.B. (1975): Refinement of the crystal structure of kröhnkite. *Acta Crystallogr.* **B31**, 1753-1755.

HERWIG, S. & HAWTHORNE, F.C. (2006): The topology of hydrogen bonding in brandtite, collinsite and fairfieldite. *Can. Mineral.* **44**, 1181-1196.

HUMINICKI, D.M.C. & HAWTHORNE, F.C. (2002): The crystal chemistry of the phosphate minerals. *In* Phosphates: Geochemical, Geobiological, and Materials Importance (M.L. Kohn, J. Rakovan & J.M. Hughes, eds.). *Rev. Mineral. Geochem.* **48**, 123-253.

INTERNATIONAL TABLES FOR X-RAY CRYSTALLOGRAPHY (1992): Volume C. Kluwer Academic Publishers, Dordrecht, The Netherlands.

JAHN, H.A. & TELLER, E. (1937): Stability of polyatomic molecules in degenerate electronic states. I. Orbital degeneracy. *Proc. R. Soc., Ser. A* **161**, 220-235.

KAMPF, A.R. & MOORE, P.B. (1976): The crystal structure of bermanite, a hydrated manganese phosphate. *Am. Mineral.* **61**, 1241-1248.

KOLITSCH, U. & FLECK, M. (2005): Second update on compounds with kröhnkite-type chains. *Z. Kristallogr.* **220**, 31-41.

MOORE, P.B. & ARAKI, T. (1974): Pinakiolite, $Mg_2Mn^{3+}O_2[BO_3]$; warwickite, $Mg(Mg_{0.5}Ti_{0.5})O[BO_3]$; wightmanite, $Mg_5(O)(OH)_5[BO_3]\bullet nH_2O$: crystal chemistry of complex 3Å wallpaper structures. *Am. Mineral.* **59**, 985-1004.

SHANNON, R.D. (1976): Revised effective ionic radii and systematic studies of interatomic distances in halides and chalcogenides. *Acta Crystallogr.* **A32**, 751-767.

SHELDRICK, G.M. (1997): SHELX–97: *Program for the solution and refinement of crystal structures*. Siemens Energy and Automation, Madison, Wisconsin.

SHELDRICK, G.M. (1998): SADABS *User Guide*, University of Göttingen, Göttingen, Germany.

WILDNER, M. & STOILOVA, D. (2003): Crystal structures and crystal chemical relationships of kröhnkite- and collinsite-type compounds $Na_2Me^{2+}(XO_4)_2\bullet 2H_2O$ (X = S, Me = Mn, Cd; and X = Se, Me = Mn, Co, Ni, Zn, Cd) and $K_2Co(SeO_4)_2\bullet 2H_2O$. *Z. Kristallogr.* **218**, 201-209.

Received June 5, 2008, revised manuscript accepted January 10, 2009.